Check for updates

GDCh Research Article Angewandte International Edition Chemie www.angewandte.org

How to cite: *Angew. Chem. Int. Ed.* **2026**, *65*, e20339
doi.org/10.1002/anie.202520339

Energy Transfer Photocatalysis

Aminoboranes as Rationally Tuned Organic Photosensitizers for Energy Transfer Catalysis

*Nunzio Matera, Alessio Bussolari, Michele Mancinelli, Roberta Coccia[+], Nicolò Santarelli[+], Andrea Pellegrini, and Andrea Mazzanti**

Dedicated to Prof. L. Lunazzi on the occasion of his 85th birthday

Abstract: We report a new class of rationally designed organic photosensitizers based on boron–nitrogen-substituted scaffolds, capable of mediating challenging triplet energy transfer (EnT) reactions under visible-light irradiation. Guided by DFT and TD-DFT calculations, we modulated the twisted intramolecular charge transfer (TICT) character of the excited state through strategic substitution on the carbazole–borane framework, allowing fine-tuning of both absorption and triplet energy levels ($E_T = 63$–70 kcal mol^{-1}). The most effective catalyst outperformed traditional Ir- and xanthone-based sensitizers across benchmark EnT reactions, including E/Z isomerizations, [2 + 2] photocycloadditions, and [1,3]-sigmatropic rearrangement. This B–N system enables the sensitization of coumarin-related substrates with $E_T \geq 65$ kcal mol^{-1}, which was previously inaccessible to fully organic EnT photocatalysts. These results establish a new design principle for modular, high-energy triplet sensitizers based on organic aminoborane scaffolds.

Introduction

Triplet energy transfer (EnT) catalysis has become a key strategy in visible-light-driven photochemistry, enabling selective substrates excitation via triplet sensitization.[1,2] However, the design of efficient, tunable, and higher triplet-state energy sensitizers remains challenging. Traditional photocatalysts often rely on metal complexes,[3–6] which offer great tunability in terms of triplet energies, catalyst loading, and absorption in the visible region. Prominent examples from the groups of Wenger and Nolan illustrate the versatility of such systems (Figure 1a).[4–6]

In contrast, fully organic sensitizers offer a more sustainable alternative, yet the development of efficient, tunable, and high-energy organic triplet sensitizers has been hampered by intrinsic structural limitations. Known effective organic sensitizers to date -benzophenone, thioxanthone, and related carbonyl-containing compounds—derive their performance largely from the inherently high triplet energy of the carbonyl moiety (Figure 1b).[7,8] Exploring unconventional molecular

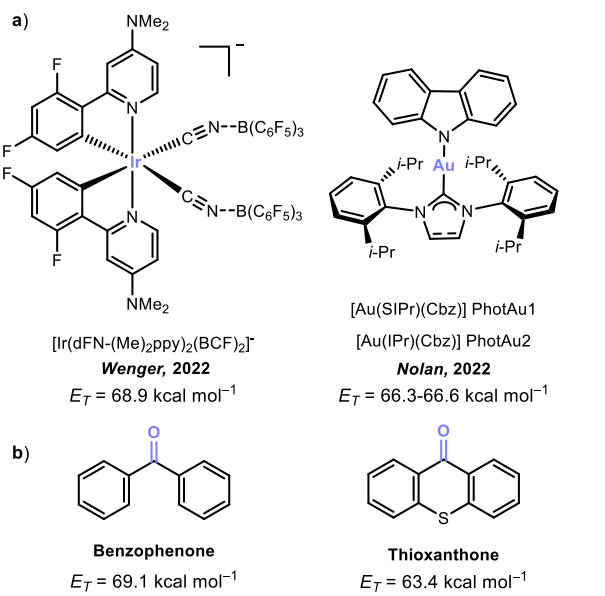

Figure 1. a) Wenger's isocyanoborato iridium (III) complex and Nolan's PhotAu complexes; b) Common organic sensitizers; c) New class of B–N based triplet sensitizers for EnT.

[*] N. Matera, A. Bussolari, M. Mancinelli, R. Coccia[+], N. Santarelli[+], A. Pellegrini, A. Mazzanti
Department of Industrial Chemistry 'Toso Montanari', University of Bologna, via Piero Gobetti, Bologna 85–40129, Italy
E-mail: andrea.mazzanti@unibo.it

[+] Both authors contributed equally to this work.

[Correction added on 16 May 2026, after first online publication: The copyright line was changed.]

Additional supporting information can be found online in the Supporting Information section

© 2025 The Author(s). Angewandte Chemie International Edition published by Wiley-VCH GmbH. This is an open access article under the terms of the Creative Commons Attribution License, which permits use, distribution and reproduction in any medium, provided the original work is properly cited.

© 2025 The Author(s). Angewandte Chemie International Edition published by Wiley-VCH GmbH

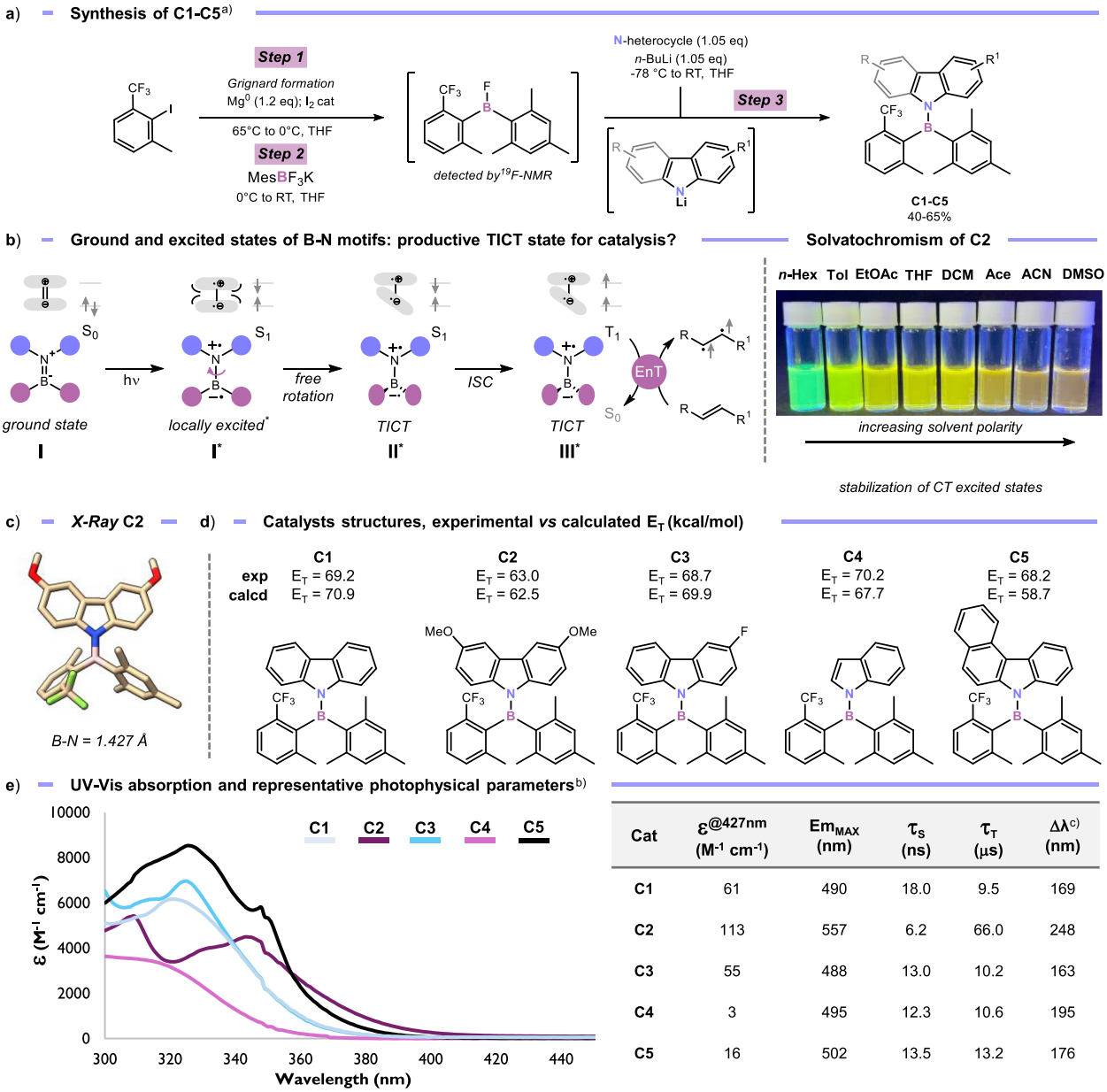

Cat	ε@427nm (M^{-1} cm^{-1})	Em_{MAX} (nm)	τ_S (ns)	τ_T (μs)	Δλ[c)] (nm)
C1	61	490	18.0	9.5	169
C2	113	557	6.2	66.0	248
C3	55	488	13.0	10.2	163
C4	3	495	12.3	10.6	195
C5	16	502	13.5	13.2	176

Figure 2. a) Synthesis of PCs **C1-C5**; b) Left: hypothesis of active species during sensitization; Right: catalyst **C2** solvatochromism in solvents of increasing polarity (10^{-4} M solutions; excited with a 366 nm portable UV lamp); c) X-ray structure of **C2**; d) Catalysts **C1-C5** structures and experimental triplet energies (glass matrix of THF, phosphorescence at 77 K) versus calculated values (DFT ωB97X-D/6–311G(d,p) [IEF-PCM(THF)]); e) Left: UV–vis absorption profiles of **C1** (light blue) **C2** (dark purple) **C3** (cyan) **C4** (light purple) **C5** (black) in 10^{-4} M THF solutions; Right: Table of photo-physical parameters. [a)] For synthesis details, characterization and screening of this class of compounds see Section 3.1 of the Supporting Information. [b)] Photophysical data of PCs in Section 3.2 of the Supporting Information. [c)] Stokes shift derived from the difference of maximum of emission and absorption of 10^{-4} M THF solutions.

scaffolds that depart from this established motif therefore represents a promising avenue toward the next generation of organic triplet sensitizers.[9,10] In this regard, boron–nitrogen (B–N) substitution has shown great promise in optoelectronic materials by enabling control over excited-state energies and emission properties.[11,12] While their application in EnT catalysis remains largely underexplored, one notable exception is Wang's report of a boron carbonitride-based system employed in a Birch-type photoreduction via consecutive triplet sensitization and electron transfer.[13] However, a general strategy for the design of modular, tunable organic B–N-based EnT photocatalysts is still lacking. Herein, we report a class of aminoborane-based organic photosensitizers capable of triplet sensitization of high-energy substrates under visible light irradiation, enabled by a structure-guided design that leverages twisted intramolecular charge transfer (TICT) to promote intersystem crossing and fine-tune photophysical properties. In particular, bisaryl-boryl-*N*-heterocyclic

© 2025 The Author(s). Angewandte Chemie International Edition published by Wiley-VCH GmbH

15213773, 2026, 5, Downloaded from https://onlinelibrary.wiley.com/doi/10.1002/anie.202520339 by Area Sistemi Dipart & Doc, Wiley Online Library on [21/05/2026]. See the Terms and Conditions (https://onlinelibrary.wiley.com/terms-and-conditions) on Wiley Online Library for rules of use; OA articles are governed by the applicable Creative Commons License

compounds emerge as promising candidates, providing a blueprint for rational design of organic photocatalysts for demanding visible-light-driven transformations (Figure 1c).

Results and Discussion

Background and Photocatalyst Design

Building on our previous carbazole–borane studies, we exploited the unique electronic features of the B–N bond to design tunable, *high-energy* organic photosensitizers.[14,15] The synthesis of the photocatalysts (PCs) proceeds through a simple and scalable three-step organometallic sequence, affording compounds **C1**–**C5** in moderate to good yields (40%–65%; see Figure 2a). As C=C double bonds isosteres, B–N units exhibit significant ground-state π character, as confirmed by the X-ray structure of catalyst **C2** (Figure 2c). Upon photoexcitation, these bonds undergo a twisted intramolecular charge transfer (TICT) process, providing highly polarized excited states—a behavior evidenced by large Stokes shifts (163–248 nm, Figure 2e) and pronounced solvatochromism (Figure 2b).[16,17] The TICT configuration is expected to enhance intersystem crossing (ISC) efficiency due to increased charge separation, a feature known to promote triplet formation.[18,19] Our design plan posits that photoexcited **I*** transitions form a locally excited singlet state to a TICT singlet state **II*** via single-bond rotation, driven by steric effects. The resulting triplet state (**III***) acts as the active species for EnT (Figure 2b). To validate and exploit our design plan, we engineered molecular scaffolds to precisely modulate charge transfer (CT) separation in the excited state.[20] Specifically, we selected substituents to either enhance or attenuate the CT features. By incorporating electron-donating or electron-withdrawing substituents on the carbazole moiety (compounds **C1–C3**) and modifying the extent of ring conjugation (compounds **C4–C5**), we tailored the electronic properties of the catalysts. These modifications resulted in modular triplet energies (E_T = 63.0–70.2 kcal mol^{-1}; Figure 2d).

The UV–vis absorption spectra of **C1–C5** are presented in Figure 2e, with **C2** exhibiting the highest molar absorptivity in the visible region (ε = 113 M^{-1} cm^{-1} at 427 nm) and the largest red-shifted emission (λ_{max} = 557 nm). The accompanying table lists photophysical parameters for **C1-C5** catalysts, including triplet lifetimes (τ_T) from 9.5 to 66.0 µs and Stokes shifts ($\Delta\lambda$) from 169 to 248 nm (Figure 2e).

Isomerization of Dimethyl Fumarate 1a-E

We then evaluated the EnT capabilities of the new boron–nitrogen-based sensitizers **C1-C5** for $E \rightarrow Z$ isomerization of fumarate **1a-*E*** (E_T = 66.0 kcal mol^{-1}) to maleate **1a-*Z*** (E_T = 71.0 kcal mol^{-1}), a benchmark for EnT catalysis (Figure 3).[2,21] Despite having the lowest triplet energy in the series (E_T = 63.0 kcal mol^{-1}; Figure 2d), catalyst **C2** was the most effective under 427 nm irradiation, outperforming catalysts **C1** and **C3-C5**. Under optimized conditions (5 mol% **C2**, *n*-hexane, 440 nm irradiation, 8 h), a 4:96 *E:Z* isomer ratio was obtained with full mass recovery. Control experiments confirmed that no isomerization occurred in the absence of either light or catalyst (entry 2). Irradiation at 456 nm proved detrimental, reducing the *E:Z* ratio to 52:48 (entry 4). Other photocatalysts (**C1**, **C3-C5**) showed no activity at 440 nm (entry 5) and only marginal performance at 427 nm (entry 6). Benchmark sensitizers, including an iridium-based EnT catalyst and thioxanthone, were also tested under identical conditions and consistently underperformed compared to **C2** (entries 7 and 8; see Section 4.1 of the Supporting Information for comprehensive screening data).

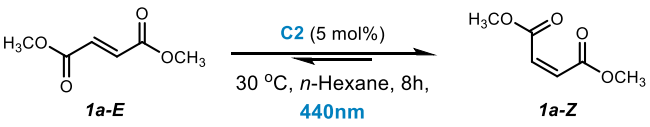

1a-E (E_T = 66 Kcal/mol) **1a-Z** (E_T = 71 Kcal/mol)

Entry	Deviation	*E:Z*[a]	Yield(*Z*)[a]
1	none	**4:96**	96
2	no catalyst, no light	>99:1	traces
3	16h or 24h	4:96	96
4[b]	456nm instead of 440nm	52:48	48
5[b]	**C1, C3-C5** instead of **C2**	>99:1	traces
6[b]	**C1, C3-C5** instead of **C2** (427nm)	<85:15	15
7[b]	[Ir][c] (1% mol) instead of **C2**	77:23	23
8[b]	THX (5% mol) instead of **C2**	>99:1	traces

Figure 3. Optimization of dimethyl fumarate (**1a-*E***) *E:Z* isomerization. Reactions were conducted on 0.1 mmol scale, 100 mM concentration. [a] The *E:Z* isomer ratio and **1a-*Z*** yields were determined by ^{1}H-NMR analysis using dibromomethane as internal standard. Full mass recovery and absence of side products were confirmed for entries 1–8. [b] Irradiation for 16 h instead of 8 h. [c] (Ir[dF(CF$_3$)ppy]$_2$(dtbpy))PF$_6$.

Computational Insights into C2 TICT State

To elucidate the electronic and structural properties of the ground and excited states involved in the photoexcitation of catalyst **C2**, we performed DFT and time-dependent DFT (TD-DFT) calculations at the CAM-B3LYP/6–311G(d,p) level of theory with a polarizable continuum model [IEF-PCM (THF)]. Building on our prior studies of twisted carbazole-borane systems, which provided insights into their stereochemical features,[14] we examined all the available conformations of **C2**. The results are summarized in Figure 4 for the more stable conformation (a detailed analysis of catalysts **C1–C5** is provided in Section 3.3 of Supporting Information). In the ground state (S_0), the B–N fragment exhibits significant double-bond character, with a bond length of 1.433 Å and a dihedral angle (φ) of 27.4° (1.427 Å and 29° in the X-ray structure). Vertical excitation, primarily involving the HOMO–LUMO transition (Figure 4b –bottom table), generates a locally excited (LE) state, which upon relaxation yields S_1 geometry.

This excited state is consistent with a twisted intramolecular charge transfer configuration, characterized by a slightly elongated B–N bond (1.537 Å) and a significantly increased dihedral angle (φ = 56.7°). The triplet state (T_1) geometry is comparable to S_1, with a similar B–N bond length (1.545 Å)

© 2025 The Author(s). Angewandte Chemie International Edition published by Wiley-VCH GmbH

15213773, 2026, 5, Downloaded from https://onlinelibrary.wiley.com/doi/10.1002/anie.202520339 by Area Sistemi Dipart & Doc, Wiley Online Library on [21/05/2026]. See the Terms and Conditions (https://onlinelibrary.wiley.com/terms-and-conditions) on Wiley Online Library for rules of use; OA articles are governed by the applicable Creative Commons License

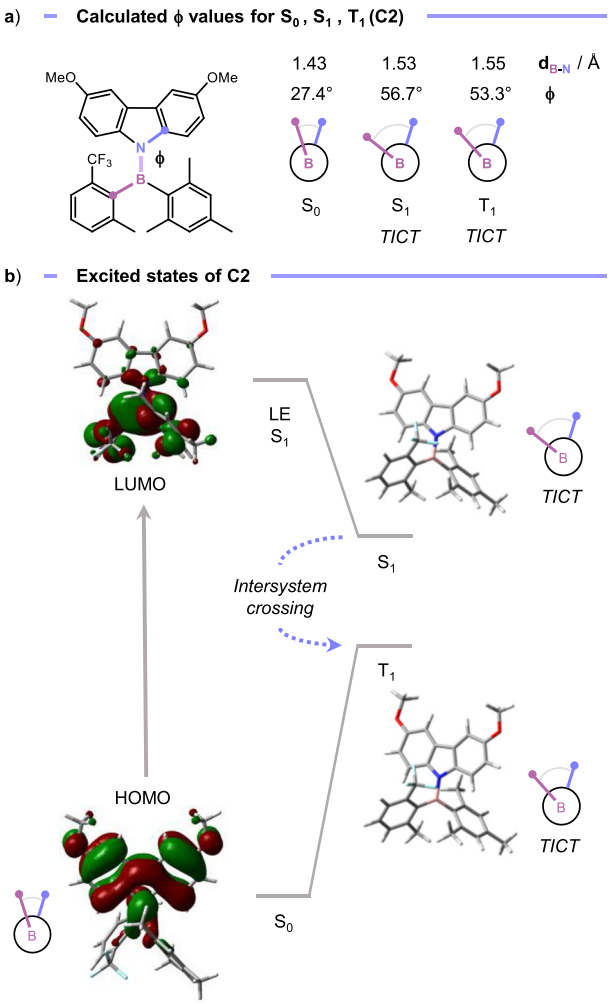

	calcd kcal/mol (eV)	exp kcal/mol (eV)
$\Delta(S_1\text{-}T_1)^{a)}$	2.33 (0.10)	1.4 (0.06)
$\Delta(T_1\text{-}S_0)^{a)}$	61.4 (2.66)	63.0 (2.73)
Transition (%)	**Excitation**	**f**
HOMO → LUMO (77)	308 nm	0.3976
HOMO(-1) → LUMO (+1) (84)	274 nm	0.3879

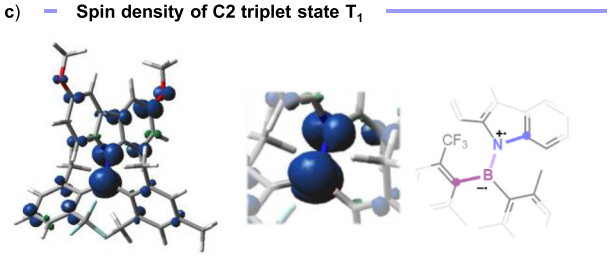

Figure 4. a) Computed dihedral angles (C_q-B-N-C_q) for the optimized S_0, S_1, T_1 geometries of **C2**. b) top: Excited state diagram of **C2** showing vertical absorption and optimized geometries for S_1 and T_1 states; bottom: comparison between computational and experimental data, including the most populated transitions (%), corresponding excitation wavelength and oscillator strength (f). c) Spin density of **C2** in the T_1 state. [a] CAM-B3LYP/def2-TZVPPD//r^{2}SCAN-3c [CPCM(THF)] (ΔG values).

and dihedral angle (φ = 53.3°), suggesting that T_1 also adopts a TICT configuration. Moreover, the calculated triplet energy (E_T) values and singlet-triplet energy gaps $\Delta G(S_1–T_1)$ are in good agreement with experimental data, further corroborating the effectiveness of the computational analysis. The spin density distribution of the T_1 state (Figure 4c) reveals that the majority of it resides on the polarized B–N bond, supporting the biradicaloid nature of this moiety. These computational results indicate that the B–N fragment plays a crucial role in the catalyst EnT activity, underscoring its function as the key catalytic species.

EnT Benchmarks and Synthetic Applications

To evaluate the effectiveness of **C1-C5** in EnT catalysis, we investigated their performance in a series of known and challenging photochemical transformations (Figure 5a). Our initial target was the *E*/*Z* isomerization of oxime **1b-*E*** (E_T = 59.0 kcal mol^{-1}) to **1b-*Z*** (E_T = 72.0 kcal mol^{-1}).[22] This reaction has been previously reported using an iridium-based sensitizer under 427 nm irradiation.[23] Employing optimized reaction conditions, catalyst **C2** achieved partial selectivity for the *Z*-isomer, yielding a *Z*:*E* ratio of 81:19 at 440 nm. Subsequently, we explored the more demanding [2 + 2] cycloaddition of norbornadiene (NBD, **1c**, E_T = 62.1 kcal mol^{-1}) to quadricyclane (QD, **2c**).[7] This transformation proceeded with moderate reactivity to afford **2c** in 78% yield after 3 h of irradiation of **C1** at 370 nm. Screening of related catalysts (see Section 4.3 of the Supporting Information) revealed that **C5** also promoted the reaction efficiently under irradiation at 390 nm, providing **2c** in 57% yield after 16 h. To further challenge this catalytic system, we turned our attention to the 1,3-sigmatropic rearrangement of verbenone **1d** to chrysantenone **2d**—a benchmark transformation known for its exceptionally high energetic demand (E_T = 69.0 kcal mol^{-1}).[4,7,24,25] Control experiments established that visible-light irradiation was crucial to suppress background reactivity (see Section 4.4 of Supporting Information). Under these conditions, **C2** was examined under irradiation at 427 nm. Despite a triplet energy gap of approximately 6 kcal mol^{-1},[26] **C2** furnished **2d** in 98% yield, albeit with a somewhat reduced reaction rate.

Having validated the performance of the PCs in well-established benchmarks, we turned our attention to applications concerning [2 + 2] photocycloaddition.[27,28] For this purpose, we selected 4-hydroxycoumarin derivatives, a privileged scaffold in the pharmaceutical realm and a challenging substrate for sensitization due to its $E_T \geq$ 65.0 kcal mol^{-1}.[29–31] We envisioned that functionalization of the enolic double bond via [2 + 2] cycloaddition could furnish valuable intermediates for drug discovery. We began by screening intramolecular reactions of coumarin derivatives **3a-c**, all of which performed well under 390 nm irradiation in acetonitrile using 5% mol of **C1**, achieving products **4a-c** in yields up to 89% (Figure 5b). Next, we focused on the more challenging intermolecular [2 + 2] cycloaddition of 4-acetyloxycoumarins **5a-c** with cyclohexene, which yielded the corresponding products **6a-c** in high yields (up to 78%;

© 2025 The Author(s). Angewandte Chemie International Edition published by Wiley-VCH GmbH

15213773, 2026, 5, Downloaded from https://onlinelibrary.wiley.com/doi/10.1002/anie.202520339 by Area Sistemi Dipart & Doc, Wiley Online Library on [21/05/2026]. See the Terms and Conditions (https://onlinelibrary.wiley.com/terms-and-conditions) on Wiley Online Library for rules of use; OA articles are governed by the applicable Creative Commons License

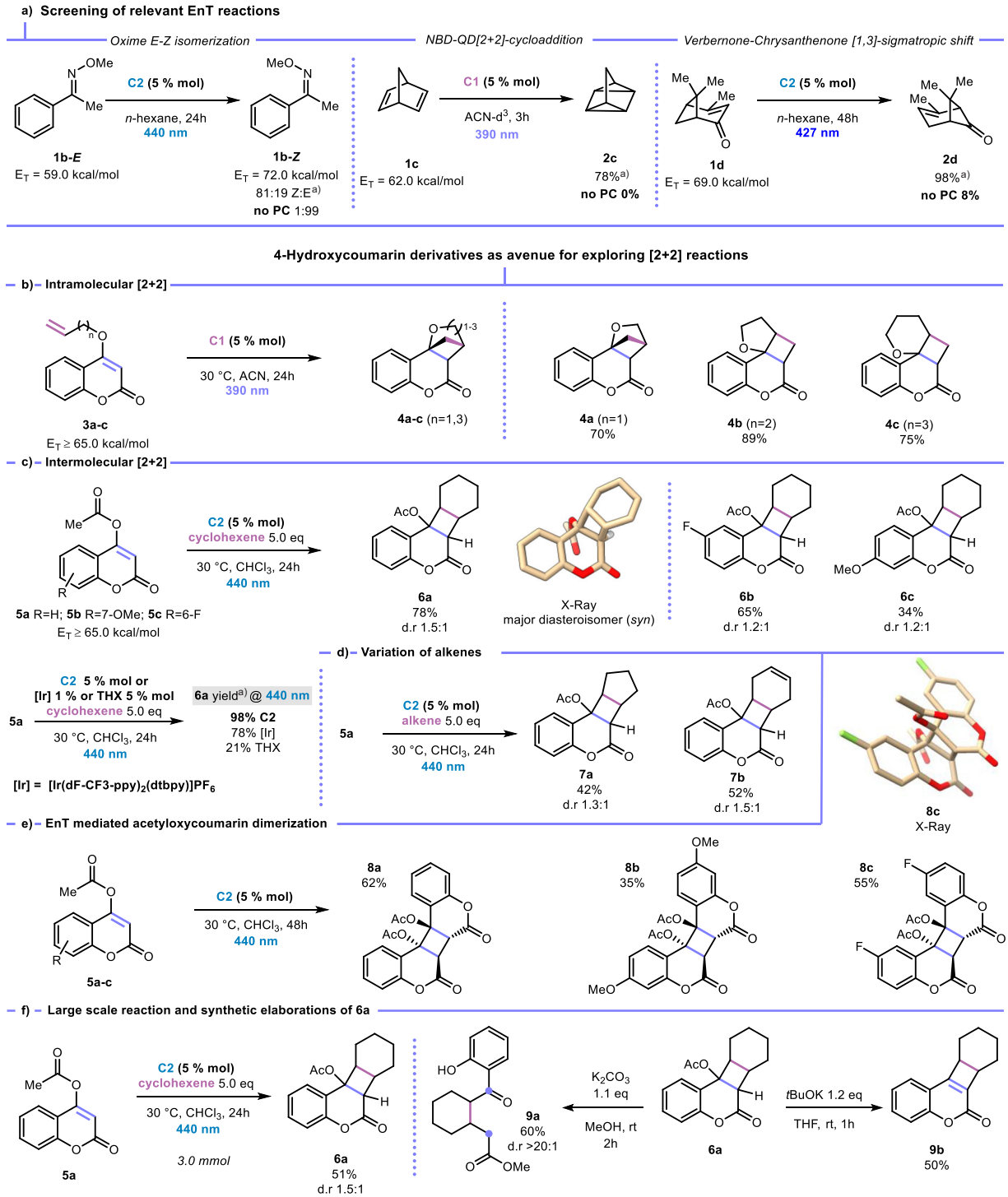

Figure 5. a) **C1**/**C2** application for common sensitization benchmarks. These reactions were conducted on a 0.1 mmol scale. b)–f) Unless otherwise noted the yields refer to isolated products after column chromatography. For the preparation and characterization of SMs and products see Supporting Information. [a)]Yields were determined via ^{1}H-NMR using dibromomethane as internal standard. For all the reactions described in this figure, photochemical setup 1 was employed (see Section 4 of Supporting Information).

Figure 5c) using 440 nm irradiation in the presence of **C2**. The *syn-anti* d.r. of these products were determined by ^{1}H-NMR spectra, and the X-ray analysis confirmed the *syn* relative configuration for the major diastereomer of product **6a** (Figure 5c). Notably, catalyst **C2** outperformed commonly used sensitizers at 440 nm (Figure 5c, bottom table) and, at 427 nm irradiation, it proved again to be the most active one among **C1-C5** (see Section 5.3 of Supporting Information for additional screening). To further demonstrate the practical value of these transformations, we also tested

© 2025 The Author(s). Angewandte Chemie International Edition published by Wiley-VCH GmbH

15213773, 2026, 5, Downloaded from https://onlinelibrary.wiley.com/doi/10.1002/anie.202520339 by Area Sistemi Dipart & Doc, Wiley Online Library on [21/05/2026]. See the Terms and Conditions (https://onlinelibrary.wiley.com/terms-and-conditions) on Wiley Online Library for rules of use; OA articles are governed by the applicable Creative Commons License

a small set of un-activated alkenes in this transformation with 4-acetyloxycoumarin **5a**, delivering products **7a** and **7b** (Figure 5d). In the absence of an inert alkene, sensitization of 4-acetyloxycoumarins **5a-c** led to the formation of dimers **8a-c** in moderate yields (Figure 5e), with regiochemistry consistent with the philicity of the generated diradical[32] (confirmed by the X-ray structure of **8c**). Additionally, following a reported procedure,[33] treatment of **6a** with potassium carbonate in methanol provided the ester **9a** in good yield, whereas the intriguing cyclobutene **9b** was obtained employing *t*-BuOK as base (Figure 5f, right). Finally, we scaled up the reaction between **5a** and cyclohexene to 3 mmol achieving a 51% isolated yield after 24 h (Figure 5f, left), with complete recovery of catalyst **C2** during the purification phase.

Photostability

Photostability is a determining parameter for photocatalysts, especially when large-scale applications or flow experiments are conducted. Motivated by the quantitative recovery of **C2** during the scale-up experiment, we investigated the photostability of the designed class of sensitizers under irradiation at 390 nm. This wavelength was chosen because of the increased absorbance across the whole PCs family (see Figure S4 of the Supporting Information). Control experiments presented in Figure 6 show that there is a similar trend of photodegradation when no sensitization occurs (Figure 6a; <40% recovered PCs after 24 h).[4]

Among the B–N photocatalysts studied at 390 nm, **C5** emerged as the most stable, likely due to its lower degree of charge-transfer (CT) character in the excited state (see Figure S14 of Supporting Information for details). However, **C2** shows markedly superior photostability at 440 nm: more than 80% of the photocatalyst was recovered after 24 h in the absence of reagents (dotted line in Figure 6a).

In contrast, when the same experiments were performed in the presence of **C1-C5** with **5a** and cyclohexene (Figure 6b), the results were dramatically different. After 16 h of irradiation, the percentage of recovered photocatalyst was quantitative in all cases, consistent with efficient excited-state quenching through energy transfer (see Section 6.3 in the Supporting Information for the optimized reaction conditions with **C2** at 440 nm).

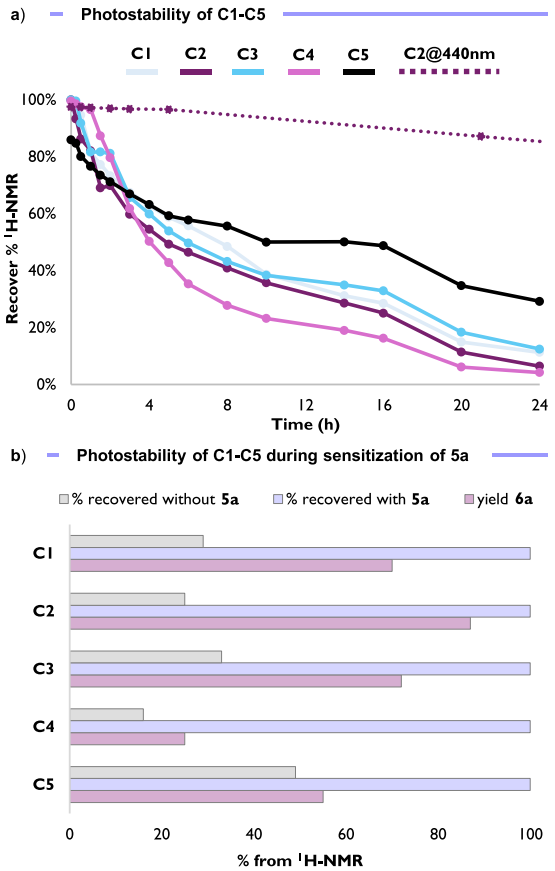

Figure 6. a) Photostability of **C1-C5** over 24 h under 390 nm irradiation in $CDCl_3$ (5 mM), in the absence of any reagent; b) Photostability of **C1-C5** during the reaction of **5a** in the presence of cyclohexene (5 eq) after 16 h of irradiation at 390 nm in $CDCl_3$. Gray bar: % recovery of **C1-C5** in the absence of reagents. Light purple bar: % recovery of **C1-C5** recovered during the sensitization of **5a**. Dark pink bar: % yield of **6a**. All reactions were performed on 0.1 mmol scale (100 mM concentration; 5% mol catalyst loading). In all cases the % of recovered PCs and the reaction yield were determined by ^{1}H-NMR using 100 mM CH_2Br_2 as the internal standard.

Conclusions

In conclusion, we have used a rational scaffold design, guided by electronic structure analysis and TICT-based mechanistic insight, to develop a new class of organic triplet photosensitizers.

By combining DFT and TD-DFT calculations with comprehensive photophysical characterization, we engineered aminoborane scaffolds with tunable UV absorption and triplet energy levels (E_T = 63–70 kcal mol^{-1}). Among them, catalyst **C2** emerged as the most effective under visible light, across a series of benchmark EnT transformations. Furthermore, **C1** and **C2** successfully mediated demanding [2 + 2] photocycloadditions of 4-hydroxycoumarin derivatives, a substrate class with high triplet energy and limited precedent in organic sensitization. These findings not only highlight the efficacy of the B–N TICT framework in promoting efficient intersystem crossing and energy transfer, but also establish it as a modular and versatile platform to access challenging photochemical transformations using fully organic photocatalysts.

Supporting Information

Details of experimental procedures and full characterization data[33] and copies of NMR spectra (PDF); The authors have cited additional references within the Supporting Information.[34–54]

© 2025 The Author(s). Angewandte Chemie International Edition published by Wiley-VCH GmbH

15213773, 2026, 5, Downloaded from https://onlinelibrary.wiley.com/doi/10.1002/anie.202520339 by Area Sistemi Dipart & Doc, Wiley Online Library on [21/05/2026]. See the Terms and Conditions (https://onlinelibrary.wiley.com/terms-and-conditions) on Wiley Online Library for rules of use; OA articles are governed by the applicable Creative Commons License

Acknowledgements

MM acknowledges financial support under the National Recovery and Resilience Plan (NRRP), Mission 4, Component 2, Investment 1.1, Call for Tender No. 1409 published on 14.09.2022 by the Italian Ministry of University and Research (MUR), funded by the European Union—NextGenerationEU- Project P2022WSJKS SiFi-MYSTERY – CUP J53D23014630001- Grant Assignment Decree No.1386 adopted on 01/09/2023. AM and MM thank the University of Bologna (RFO funds). Thanks are due to Prof. P. Melchiorre for helpful discussion.

Conflict of Interests

The authors declare no conflict of interest.

Data Availability Statement

The data that support the findings of this study are available in the Supporting Information of this article.

Keywords: Aminoboranes · Energy transfer (EnT) · Organic photocatalyst · Photochemistry

[1] F. S. Kalthoff, M. J. James, M. Teders, L. Pitzer, F. Glorius, *Chem. Soc. Rev.* **2018**, *47*, 7190–7202, https://doi.org/10.1039/C8CS00054A.
[2] S. Dutta, E. J. Erchinger, F. S. Kalthoff, R. Kleinmans, F. Glorius, *Chem. Soc. Rev.* **2024**, *53*, 1068–1089, https://doi.org/10.1039/D3CS00190C.
[3] K. Grudzień, Z. Szeptuch, H. Kubiszewski, W. Chaladaj, K. Rybicka-Jasińska, *J. Org. Chem.* **2024**, *89*, 8546–8550, https://doi.org/10.1021/acs.joc.4c00450.
[4] L. Schmid, F. Glaser, R. Schaer, O. S. Wenger, *J. Am. Chem. Soc.* **2022**, *144*, 963–976, https://doi.org/10.1021/jacs.1c11667.
[5] E. A. Martynova, V. A. Voloshkin, S. G. Guillet, F. Bru, M. Belis, K. Van Hecke, C. S. J. Cazin, S. P. Nolan, *Chem. Sci.* **2022**, *13*, 6852–6857, https://doi.org/10.1039/D2SC00864E.
[6] V. A. Voloshkin, M. Villa, E. A. Martynova, M. Belis, K. Van Hecke, P. Ceroni, S.P. Nolan, *Chem. Sci.* **2024**, *15*, 4571–4580, https://doi.org/10.1039/D3SC06675D.
[7] F. S. Kalthoff, F. Glorius, *Chem.* **2020**, *6*, 1888–1903.
[8] D. L. Elliot, S. Kayal, W. M. George, K. Booker-Milburn, *J. Am. Chem. Soc.* **2020**, *142*, 14947–14956, https://doi.org/10.1021/jacs.0c05069.
[9] S. Mallik, H. Wang, N. Matera, B. X. Li, S. Stagni, P. Melchiorre, *Angew. Chem. Int. Ed.* **2025**, *64*, e202509770.
[10] N. Hölter, N. H. Rendel, L. Spierling, A. Kwiatkowski, R. Kleinmans, C. G. Daniliuc, O. S. Wenger, F. Glorius, *J. Am. Chem. Soc.* **2025**, *147*, 12908–12916.
[11] K. S. Mellerup, S. Wang, *Trends Chem.* **2019**, *1*, 77–89, https://doi.org/10.1016/j.trechm.2019.01.003.
[12] Y. L. Zou, L. Z. Zhang, M. A. Ren, Q. X. Ran, K. J. Feng, *Theor. Chem. Acc.* **2010**, *126*, 361–369, https://doi.org/10.1007/s00214-009-0695-9.
[13] T. Yuan, L. Sun, Z. Wu, R. Wang, X. Cai, W. Lin, M. Zheng, X. Wang, *Nat. Catal.* **2022**, *5*, 1157–1168, https://doi.org/10.1038/s41929-022-00886-0.
[14] D. Pecorari, A. Mazzanti, S. Gianvittorio, S. Foschi, S. Stagni, V. Fiorini, M. Mancinelli, *Org. Chem. Front.* **2021**, *8*, 4496–4507, https://doi.org/10.1039/D1QO00715G.
[15] D. Pecorari, E. Giuliani, A. Mazzanti, S. Stagni, V. Fiorini, G. Vigarani, F. Zinna, G. Pescitelli, M. Mancinelli, *J. Org. Chem.* **2023**, *88*, 871–881, https://doi.org/10.1021/acs.joc.2c02209.
[16] T. Taniguchi, J. Wang, S. Irle, S. Yamaguchi, *Dalton Trans.* **2013**, *42*, 620–624, https://doi.org/10.1039/C2DT32134C.
[17] J. Wang, Y. Wang, T. Taniguchi, S. Yamaguchi, S. Irle, *J. Phys. Chem. A.* **2012**, *116*, 1151–1158, https://doi.org/10.1021/jp209264j.
[18] B. F. Dias, N. K. Bourdakos, V. Janus, C. K. Moss, T. K. Kamtekar, V. Bhalla, J. Santos, R. M. Bryce, P. A. Monkman, *Adv. Mater.* **2013**, *25*, 3707–3714, https://doi.org/10.1002/adma.201300753.
[19] M. S. King, R. Matheson, B. F. Dias, P. A. Monkman, *J. Phys. Chem. B.* **2008**, *112*, 8010–8016, https://doi.org/10.1021/jp712163b.
[20] T. Bortolato, G. Simionato, M. Vayer, C. Rosso, L. Paoloni, M. E. Benetti, A. Sartorel, D. Lebœuf, L. Dell'Amico, *J. Am. Chem. Soc.* **2023**, *145*, 1835–1846, https://doi.org/10.1021/jacs.2c11364.
[21] T. Nevesely, J. J. Molloy, C. McLaughlin, L. Brüss, G. C. Daniliuc, R. Gilmour, *Angew. Chem. Int. Ed.* **2022**, 61.
[22] M. Montalti, A. Credi, L. Prodi, T. M. Gandolfi, *Handbook of Photochemistry*, CRC Press, Boca Raton, FL **2006**.
[23] X. Zhang, T. Rovis, *J. Am. Chem. Soc.* **2021**, *143*, 21211–21217, https://doi.org/10.1021/jacs.1c10148.
[24] D. I. Schuster, D. Widman, *Tetrahedron Lett.* **1971**, *12*, 3571–3574, https://doi.org/10.1016/S0040-4039(01)97233-8.
[25] M. Griffin, Z. E. Colman, *ChemRxiv*., **2025**, https://doi.org/10.26434/chemrxiv-2025-t373h.
[26] Similar EnT processes with such high endergonic disadvantage between the donor and the acceptor are known in the literature F. S. Kalthoff, C. Henkel, M.c. Teders, B. Abel, M. D. Guldi, F. Glorius, *Chem*. **2019**, *5*, 2183–2194.
[27] A. Vasudevan, C. Villamil, J. Trumbull, J. Olson, D. Sutherland, J. Pan, S. Djuric, *Tetrahedron Lett.* **2010**, *51*, 4007–4009, https://doi.org/10.1016/j.tetlet.2010.05.119.
[28] H. Suginome, F. C. Liu, S. Seko, K. Kobayashi, *J. Org. Chem.* **1988**, *53*, 5952–5959, https://doi.org/10.1021/jo00260a027.
[29] J. Seixas de Melo, P. F. Fernandes, *J. Mol. Struct.* **2001**, *69–78*, 565–566.
[30] I. Manolov, C. Maichle-Moessmer, N. Danchev, *Eur. J. Med. Chem.* **2006**, *41*, 882–890, https://doi.org/10.1016/j.ejmech.2006.03.007.
[31] C. J. Jung, S. O. Park, *Molecules* **2009**, *14*, 4790–4803, https://doi.org/10.3390/molecules14114790.
[32] J. J. A. Garwood, A. D. Chen, D. A. Nagib, *J. Am. Chem. Soc.* **2024**, *146*, 28034–28059.
[33] D. J. Haywood, R. G. Hunt, C. J. Potter, S. T. Reid, *J. Chem. Soc., Perkin Trans. 1* **1977**, 2458–2461, https://doi.org/10.1039/p19770002458.
[34] Deposition numbers 2480131 (for **C1**), 2480132 (for **C2**), 2480133 (for **8c**) and 2480134 (for **6a**) contain the supplementary crystallographic data for this paper. These data are provided free of charge by the joint Cambridge Crystallographic Data Centre and Fachinformationszentrum Karlsruhe Access Structures service.

Manuscript received: September 16, 2025
Revised manuscript received: December 01, 2025
Manuscript accepted: December 02, 2025
Version of record online: December 12, 2025

© 2025 The Author(s). Angewandte Chemie International Edition published by Wiley-VCH GmbH

15213773, 2026, 5, Downloaded from https://onlinelibrary.wiley.com/doi/10.1002/anie.202520339 by Area Sistemi Dipart & Doc, Wiley Online Library on [21/05/2026]. See the Terms and Conditions (https://onlinelibrary.wiley.com/terms-and-conditions) on Wiley Online Library for rules of use; OA articles are governed by the applicable Creative Commons License